

In-plane excitation of thin silicon cantilevers using piezoelectric thin films

Glenn J T Leighton, Paul B Kirby

Department of Materials, Cranfield University, MK43 0AL, United Kingdom

Colin H J Fox

School of Mechanical, Materials and Manufacturing Engineering, University of Nottingham, Nottingham NG7 2RD, United Kingdom

This paper deals with the actuation of in-plane and out-of-plane motion of silicon cantilevers, using a single thin-film of lead zirconate titanate with a split electrode configuration. In-plane actuation is confirmed, and excellent agreement is demonstrated between theoretically predicted and experimentally measured resonant amplitudes, for the fundamental out-of-plane and in-plane modes of vibration of the fabricated test cantilevers.

Many actuation principles have been applied to micro electro mechanical system (MEMS) devices including, thermal, magnetic, piezoelectric and electrostatic. Of these, electrostatic actuation is most commonly used because the fabrication processes are relatively straight forward, using materials available at most MEMS facilities. However, electrostatic actuation has several disadvantages or limitations that might potentially be avoided by using piezoelectric actuation. Often electrostatic MEMS devices require high actuation voltages to obtain significant forces, leading to a requirement for additional circuitry when used with complementary metal oxide semiconductors, for which supply voltages are falling below 3 V. In contrast, a micro-switch with thin-film piezoelectric actuation operating at 3 V¹ has recently been demonstrated. Electrostatic actuation is capable of exciting both in-plane and out-of-plane motion depending on the configuration of the capacitor plates relative to the plane of the wafer, but separate capacitors, each with accurately maintained electrode gaps, are required for each direction. The comb-drive² is an established means of increasing the available electrostatic actuation force, but only at the expense of wafer area. Further disadvantages of electrostatic actuation are the need to accurately maintain small electrode gaps and the snap-down effect, which typically limits the motion to less than two thirds of the electrode gap.

The most common configuration for piezoelectric MEMS structures is a piezoelectric thin film, with top and bottom electrodes, deposited or grown on a substrate structure. Application of a voltage across the piezoelectric film, in combination with d_{31} action, causes in-plane stresses in the film which in turn cause out-of-plane displacement of the structure. The material with the highest electro-active coefficients that can be readily deposited in thin film form on silicon (Si) wafers is lead zirconate titanate (PZT). There have been numerous reports

of the fabrication of unimorph MEMS structures using thin film PZT, particularly of Si cantilevers in which thicknesses of the Si and PZT layers are similar, and of the characterization of the out-of-plane bending that occurs when a voltage is applied across the PZT^{3,4}. Under an alternating voltage significant displacements can be achieved using mechanical resonance of the structure in an out-of-plane mode of vibration. Such motion has been used for applications including microwave filters and mass change in chemical sensing.

A recent paper⁵ presented a theoretical analysis of the mechanics of MEMS beam structures in which in-plane actuation is achieved using a piezoelectric film on the surface of the wafer with differentially excited electrode areas. However, to date, no practical demonstration of this has been reported. In this paper we demonstrate in-plane motion excited in a MEMS device by a thin film piezoelectric layer, and make comparisons with theoretical predictions based on the analysis of Chen *et al*⁵.

The unimorph cantilevers used in this study were fabricated from silicon on insulator wafers with the PZT layer deposited on the Si device layer. The fabrication process has been previously described⁶. The PZT thin films were produced using sol gel deposition to give a film thickness of 1 μ m. Platinum was used as the bottom electrode for the growth of $\text{Pb}_{1.1}(\text{Zr}_{0.3}\text{Ti}_{0.7})\text{O}_3$. The choice of cantilever dimensions was based on the desired operating frequency (90 kHz out-of-plane and 600 kHz in-plane), which to some extent was limited by available wafer thickness and processing capability. Figure 1 shows an example of the fabricated cantilever which is the basis of the results presented in this paper. Figure 2 shows a schematic of the cross section of the cantilever. The top-surface electrode is divided into two symmetrical strips of width h . In-plane actuation is achieved by applying equal-amplitude,

anti-phase sinusoidal drive voltages to the two electrodes, causing alternating anti-phase contraction and expansion of the PZT on either side of the centerline of the cantilever. Out-of-plane excitation can be achieved with the same electrode layout by applying equal-amplitude, in-phase sinusoidal drive voltages, thus causing alternating, in-phase expansion and contraction of the upper surface of the cantilever.

The silicon cantilevers had length $350\mu\text{m}$, width $(2h+h_0) = 75\mu\text{m}$ and thickness $t_b = 10\mu\text{m}$. The PZT thickness was $t_p = 1\mu\text{m}$ and the electrode width was $h=20\mu\text{m}$. X-ray characterization revealed PZT that was highly (111) oriented in the perovskite phase with no evidence of pyrochlore. Additional evidence for complete conversion to the perovskite phase is that a dielectric constant and loss of 380 and 0.01 were measured, values which for films of this composition show high piezoelectric activity. The relevant d_{31} value is given later.

Consider now the prediction of resonant amplitudes of the specimens under in-plane and out-of-plane excitation. The key theoretical results from ⁶ are as follows. Noting the dimensions defined in figure 2, the effective in-plane actuation bending moment acting at the tip of the cantilever due to anti-phase actuation of the electrodes can be expressed as

$$M_{i-p} = \frac{E_p t_p \varepsilon_0 h [h + h_0]}{1 + \frac{E_p t_p}{12 E_b I_b} [(h_0 + 2h)^3 - h_0^3]} \quad (1)$$

Where $\varepsilon_0 = d_{31}V/t_p$ is the free piezoelectric strain and $I_b = t_b(h_0 + 2h)^3/12$. V is the actuation voltage, E_b and E_p are the Young's moduli of the substrate SI and PZT respectively.

For the case where the electrodes are excited by equal voltages of the same polarity, the effective out-of-plane actuation bending moment can be expressed as

$$M_{o-p} = \frac{\epsilon_0}{\frac{1}{E_b A_b} + \frac{t_b(t_b + t_p)}{4E_b I_b'} + \frac{1}{E_p A_p}} \frac{t_b}{2} \quad (2)$$

Where A_b , A_p are respectively the cross sectional areas of the substrate and piezoelectric material and $I_b' = (h_0 + 2h)t_b^3/12$. The analysis on which equations (1) and (2) are based neglects the mechanical effects of the electrode layers.

Using a standard modal expansion approach ⁷ in which only the fundamental bending mode is retained, it can be shown that the displacement amplitude at the tip of the cantilever when harmonic excitation is applied at the resonant frequency, ω_s of an appropriate mode of vibration can be expressed as:

$$y_{RES}(L) = \frac{M\phi'(L)}{\rho AL} \frac{Q_s}{\omega_s^2} \phi(L) \quad (3)$$

M is the relevant excitation moment given by equation (1) or (2), L and ρA are the length and effective mass per unit length and Q_s is the mechanical quality factor associated with vibration mode s , which is to be determined experimentally. $\phi(L)$ and $\phi'(L)$ are the displacement and slope of the relevant Eigen function ⁸, evaluated at the tip of the cantilever ($x=L$).

For the experimental measurements, an alternating excitation of 3 V was applied to the electrodes, phased appropriately as described earlier. The out-of-plane modal response and

mode shapes were measured using the micro-scanning laser vibrometer (MSV) of the Polytech micro motion analyzer (MMA) 300. Figure 3 shows a frequency response measurement made using anti-phase excitation voltages. For presentational purposes the acceleration response has been plotted with a logarithmic scale, which increases the prominence of the small amplitude peaks. The response has prominent peaks corresponding to resonance of the first two out-of-plane bending modes at ~90 kHz and ~558 kHz and the first twisting mode at ~824 kHz. The inset images in figure 3 show the corresponding measured mode shapes. A smaller peak is visible at ~610 kHz, which is close to the predicted frequency of the fundamental in-plane bending mode of vibration.

The natural frequencies of the observed modes were within 10% of theoretical predictions based on standard textbook analyses⁸ for uniform beams and within 1% of detailed Finite Element predictions, giving confidence that the actual test structures conformed to the design.

The fact that the 90 kHz and 558 kHz in-plane modes were excited by the nominally anti-symmetric excitation (*i.e.* anti-phase voltages applied to the electrodes) indicates the presence of slight deviations of the actual structure from the symmetric ideal. This could be due, amongst other things, to slight non-uniformity in the PZT film thickness and properties or small etching imperfections affecting the accuracy of dimensions and electrode position. The fact that the resonant peaks at 90 kHz, 558 kHz and 824 kHz are the most prominent in the frequency response shown in Figure 3 is due to the fact that the laser vibrometer was being used in a mode that detects out-of-plane motion. The appearance of the smaller 610 kHz peak corresponding to an in-plane mode is again attributable to small asymmetries in the cantilever

structure, which mean that the nominally pure in-plane mode actually contains an out-of-plane displacement component.

Using anti-phase excitation voltages, the resonance of the 610 kHz in-plane mode was studied in more detail over a ~20 kHz frequency range around 610 kHz. In-plane displacements were measured using the planar motion analyzer capability of the Polytech MMA 300. This acquires a sequence of images at different phase angles over the vibration cycle using a light emitting diode to provide strobed illumination of the sample. The images were then processed to determine the motion with a sub-pixel accuracy of ~4 nm at 50 x magnification. The resulting frequency response is shown in Figure 4, where a maximum displacement of ~17.2 μm at the cantilever tip is observed. This gives a clear indication of the actuation of significant in-plane displacement of the cantilever using a single thin film of piezoelectric material deposited on the surface of the wafer, with appropriate electrode arrangement and anti-phased excitation.

The mechanical Q -factors for the 610 kHz in-plane mode was estimated using the half-power bandwidth of the frequency response curve in Figure 4 where the centre frequency is 610.6 kHz and the bandwidth is 0.18 kHz, giving $Q_{610} = 3392$. From a similar test using 3 V in-phase excitation to excite the 90 kHz out-of-plane mode it was found that the resonant displacement amplitude at the tip was 4.7 μm and that $Q_{90} = 75$.

The d_{31} piezoelectric coefficient was determined experimentally using the MSV as described in ⁴ and it was found that $d_{31}=22 \times 10^{-12} \text{m/V}$. Based on the nominal specimen dimensions, the measured values of Q , d_{31} and natural frequency ω_s , and assuming 3 V excitation, equations (1) - (3) were used to predict the resonant amplitudes at the cantilever tip for the 90 kHz (out-of-plane) and 610 kHz (in-plane) modes. Table 1 shows the predicted and measured values. For the out-of-plane mode there is excellent agreement (within 2.2%) between the measured and predicted response amplitudes. For the in-plane mode the agreement is less good but is still within 20%. In this case the previously mentioned effects of slight warping or imperfection in the structure and the relative difficulty in measuring in-plane displacements as compared to measuring out-of-plane displacements are factors that contribute to the reduced level of agreement.

Out-of-plane modes have been demonstrated by many workers and equation (3) can be regarded as a well established theoretical result. The level of agreement for the out-of-plane mode therefore gives confidence in the measured parameters as well as the validity of equation (2). For the in-plane mode, in addition to the practical demonstration of strong actuation, the level of agreement between measured and predicted amplitudes gives confidence in the validity of the previously untested equation (1) as a useful tool for design calculations.

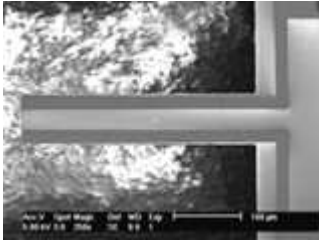
The authors acknowledge the financial support of the European Union through European Projects 027926 “Q2M” and 507352 “AMICOM”.

- ¹H.-C. Lee, J.-Y. Park and J.-U. Bu, IEEE Microw. Wirel. Compon. Lett. **15**, 202 (2005).
- ²W. C. Tang, T. H. Nguyen and R. T. Howe, IEEE Micro Electro Mech. Syst. 53 (1989)
- ³P. B. Kirby, R.V. Wright, P. Gaucher, P. Galtier, L. Kofoed, J. O. Gullov, W. Von Munch, D. Eichner, B. Ploss and J. K. Kruger, J. Phys. IV. **8**, 161 (1998).
- ⁴Z. Huang, Q. Zhang, S. Corcovic, R. A. Dorey, F. Duval, G. Leighton, R. Wright, P. Kirby and R. W. Whatmore, J Electroceram. **17**, 549 (2006).
- ⁵X. Chen, C. Fox and S. McWilliam, Proc. SPIE **5049**, 371 (2003).
- ⁶H. W. Jiang, P. Kirby and Q. Zhang, Proc. SPIE **4979**, 165 (2003).
- ⁷G. B. Warburton, *The Dynamical Behaviour of Structures* 2nd Ed (Pergamon International, Oxford, 1976).
- ⁸R. D. Blevins, *Formulas for natural frequency and mode shape* (Krieger Publishing company, 1979).

Table I Comparison of measured and theoretical resonant response amplitudes

	Measured amplitude (μm)	Predicted amplitude (Eqn (1)–(3)) (μm)
In-plane mode at 610 kHz	17.2	20.5 ^(a)
Out-of-plane mode at 90 kHz	4.7	4.8 ^(b)

(a) Based on equations (1) and (3). ^(b) Based on equations (2) and (3)



(b) Figure 1 SEM image of cantilever specimen

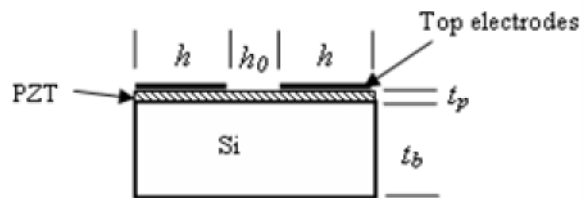


Figure 2 Schematic cross section of cantilever

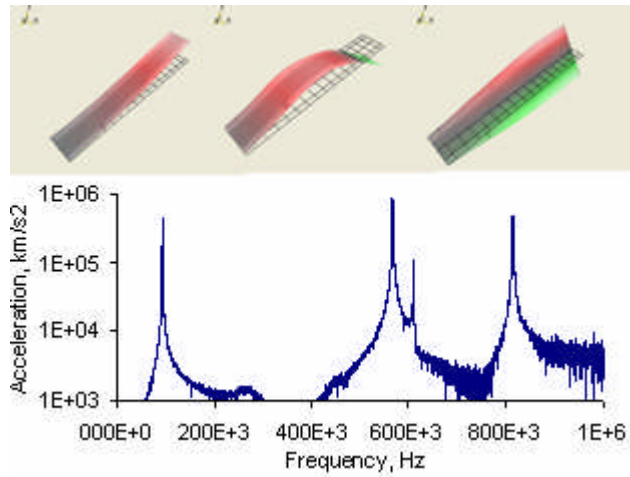


Figure 3 Frequency response of cantilever specimen, inset images show mode shapes of the 1st, 2nd and 4th modes

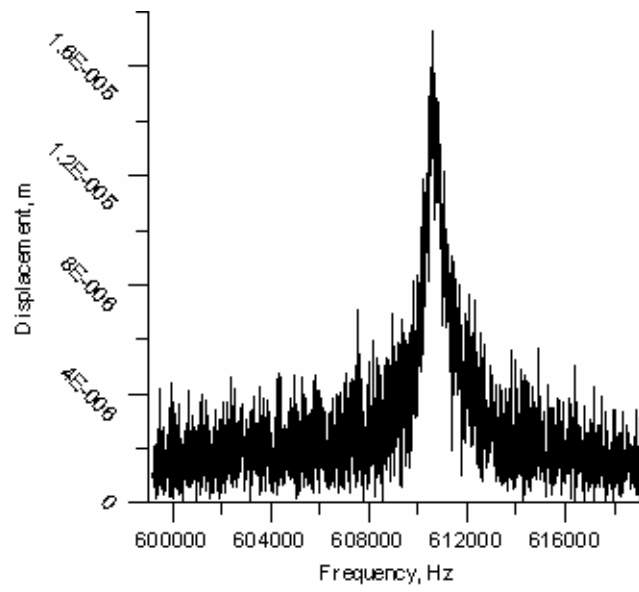


Figure 4 Frequency response of in-plane mode with description of Q determination